Supplemental Figures

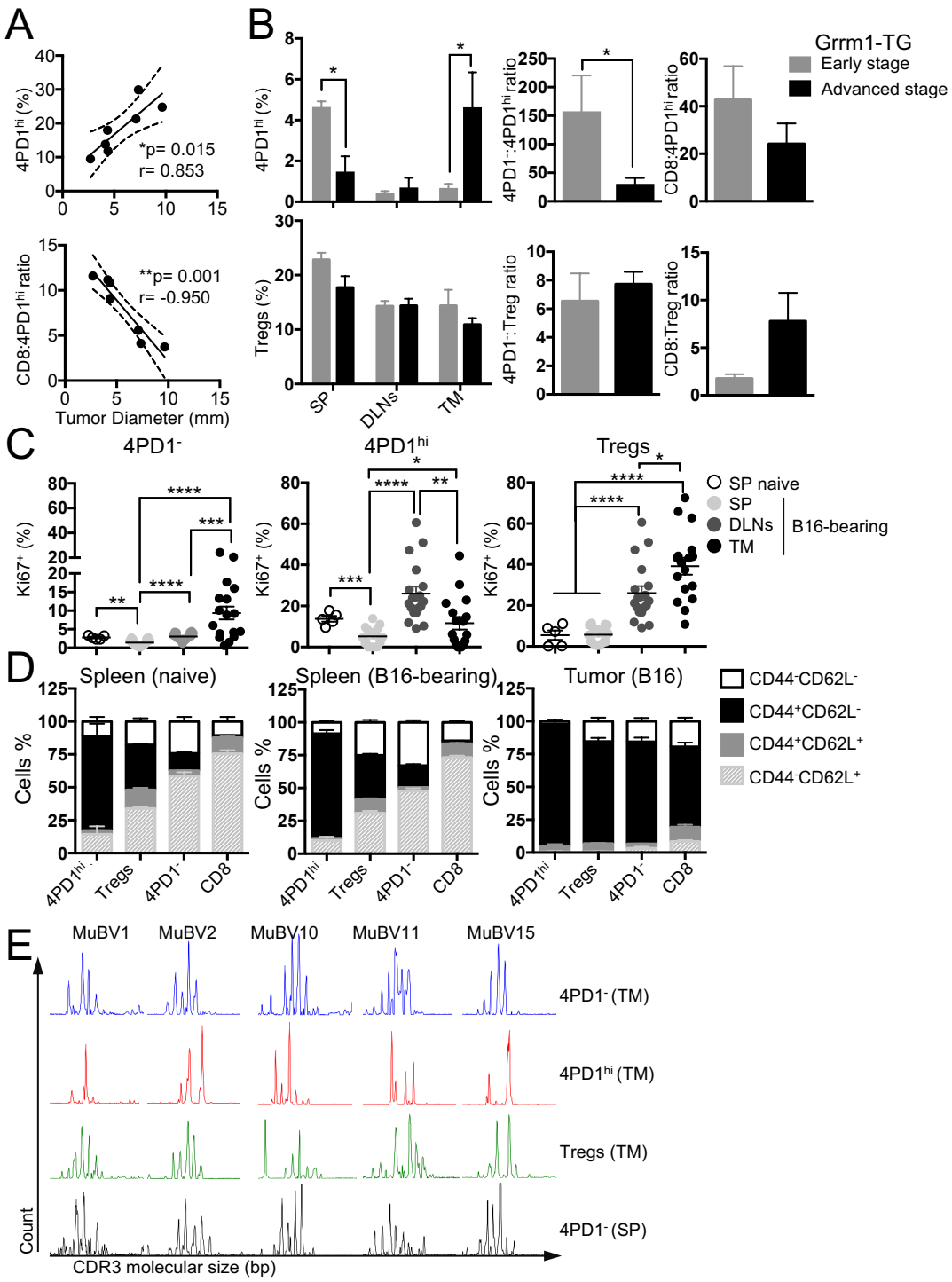

Figure S1. Related to Figure 1. 4PD1^{hi} accumulate at the tumor site with tumor progression and are antigen-experienced T cells. (A) Correlation of tumor burden with intra-tumor 4PD1^{hi} frequency and CD8:4PD1^{hi} ratio in mice injected with the same amount of B16 cells (10^5 cells). P values and Pearson r correlation coefficients are reported on the graphs. (B) Frequency of 4PD1^{hi} and Tregs in spleen (SP), tumor-draining lymph nodes (DLNs) and tumor (TM), and ratios between the indicated T-cell subsets at the tumor site in

Grm1-TG spontaneous melanoma mouse model at an early (3 months old; mean ± SEM; n=3) or advanced (6 months old; mean ± SEM; n=5) stage of melanoma development (unpaired t test). FACS analysis of Ki67 (C), CD44 and CD62L (D) expression in the indicated cell subsets and anatomic locations in naive and B16-bearing mice as in Figure 1A (mean ± SEM; unpaired t test). (E) Examples of CDR3 spectratypes (TCRBV1, TCRBV2, TCRBV10, TCRBV11 and TCRBV15; Table S1) in $4PD1^{hi}$, Tregs and $4PD1^{-}$ sorted from tumors (TM) of B16-bearing Foxp3-GFP transgenic mice. The same analysis in $4PD1^{-}$ isolated from naive spleens (SP) is reported as control. * = $p<0.05$, ** = $p<0.01$, *** = $p<0.001$, **** = $p<0.0001$.

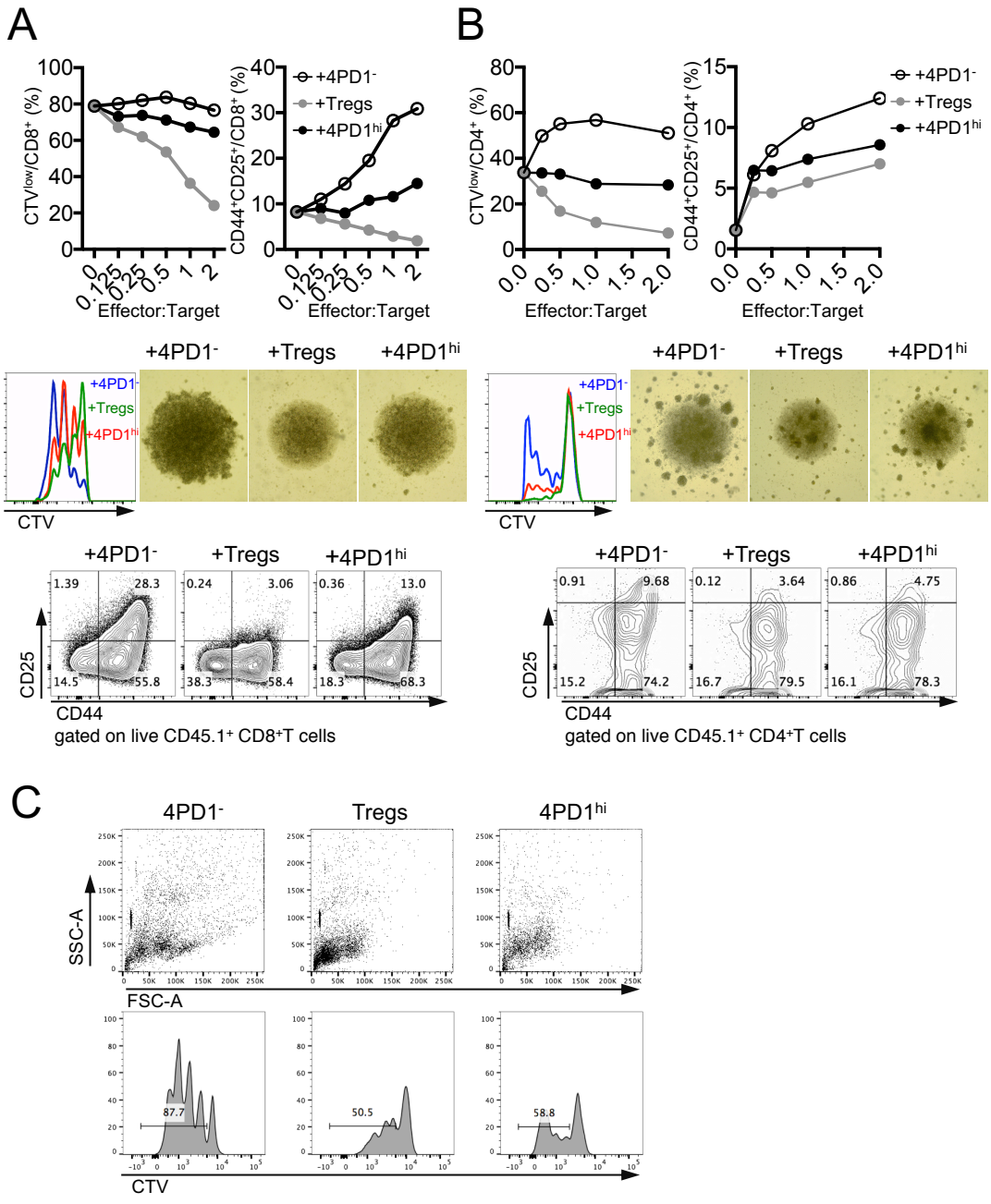

Figure S2. Related to Figure 2. Mouse 4PD1^{hi} limit T-cell effector functions. (A,B) 4PD1^{hi}, 4PD1^{-} and conventional Tregs were FACS-sorted from spleens of naive non-tumor-bearing Foxp3-GFP transgenic mice and tested in suppression assays at the indicated ratios as described in Figure 2A. Data show the results of two additional independent experiments using as target CTV-labeled CD45.1^{+} CD8^{+} (A) or CD4^{+} (B) T cells (1x10^{5} cells/condition). Proliferation and activation of target cells were measured by FACS analysis of respectively CTV dilution and frequency of CD44^{+}CD25^{+} cells after 48- (A) or 72-hr culture (B). Representative FACS plots and pictures show results from co-cultures at 1:1=effector:taregt ratio. (C) Proliferation capacity of spleen-derived 4PD1^{-}, Tregs and 4PD1^{hi} after 72-hr stimulation with anti-CD3/CD28 coated beads.

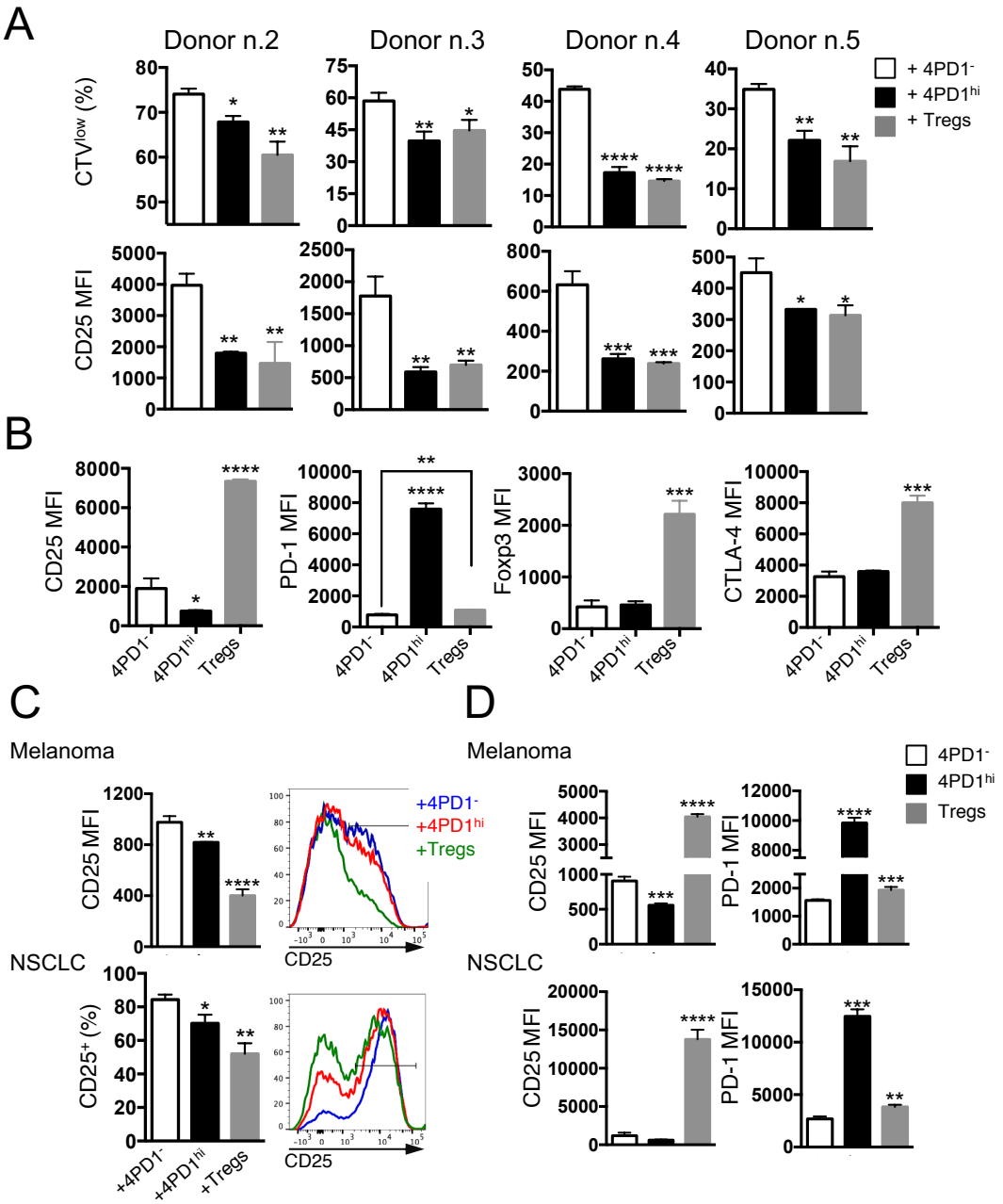

Figure S3. Related to Figure 3. Human 4PD1^{hi} limit T-cell effector functions. (A) Effects of circulating 4PD1^{hi} and Tregs in comparison with 4PD1^{-} from 4 additional healthy donors on proliferation (CTV^{low} %) and activation (CD25 MFI) of autologous target CD4^{+} T cells (1:1 ratio) after 72-hr co-culture (mean ± SD; n=2-3; unpaired t test, 4PD1^{hi} and Tregs vs 4PD1^{-}). (B) Phenotype of donor-derived effector CD4^{+} T-cell subsets (4PD1^{hi}, Tregs and 4PD1^{-}) after *in vitro* culture with target CD4^{+} T cells for 72 hr as in Figure 3A (mean ± SD; n=3; unpaired t test, 4PD1^{hi} and Tregs vs 4PD1^{-}). (C) CD25 expression (MFI or frequency of positive cells) in tumor-derived target CD4^{+} T cells and (D) phenotypic analysis of tumor-derived effector CD4^{+} T-cell subsets from *in vitro* suppression assays shown in Figure 3B (mean ± SD; unpaired t test, 4PD1^{hi} and Tregs vs 4PD1^{-}). * = p<0.05, ** = p<0.01, *** = p<0.001, **** = p<0.0001. Auto, autologous.

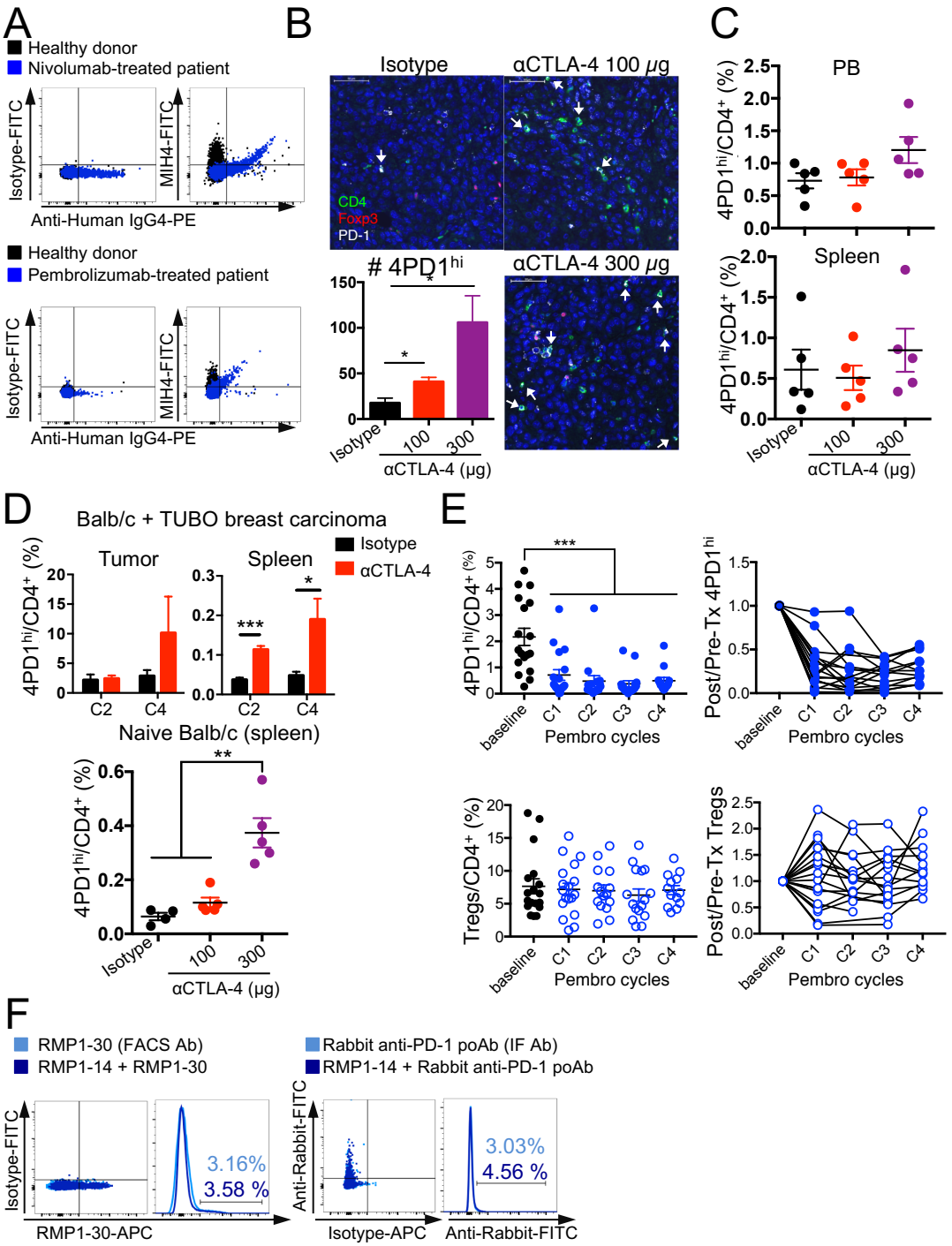

Figure S4. Related to Figure 4. 4PD1^{hi} modulation by immune checkpoint blockade. (A) Analysis of cross-reactivity between therapeutic and detection anti-human PD-1 Abs. Peripheral blood mononuclear cells (PBMC) from a healthy donor and a nivolumab- (top) or a prembrolizumab-treated patient (bottom) were co-stained with a PE-labeled anti-human IgG4 (to detect therapeutic anti-PD-1 Abs) and the FITC-labeled anti-human PD-1 used in flow cytometry analyses (MIH4) or the matched isotype IgG. Plots represent the overlay of live single CD4^{+} T cells between donor (black) and patients' (blue) samples. (B-D) αCTLA-4-dose- and tumor-dependent modulation of 4PD1^{hi}. (B) B16-melanoma-bearing C57BL/6J mice were treated with αCTLA-4 monotherapy (100 μg or 300 μg) or control isotype IgG (300 μg) as shown in Figure 4B,

and, one day after treatment completion, tumor biopsies were collected and subjected to immunofluorescent staining of CD4 (AlexaFluor488, green), Foxp3 (AlexaFluor568, red) and PD-1 (AlexaFluor647, white). Representative staining of $4PD1^{hi}$ (indicated by arrows; scale bar, 50μm; 40x original magnification) and quantification of $4PD1^{hi}$ in 3 tumors/group (mean ± SEM; unpaired t test). (C) Non-tumor-bearing C57BL/6J mice were treated with 4 courses of αCTLA-4 (100 μg or 300 μg) or the matched isotype IgG (300 μg), and, one day after treatment completion, $4PD1^{hi}$/CD4 % was measured in PB and spleen by FACS (mean ± SEM; n=5). (D) TUBO-breast-carcinoma-bearing (top) or naive Balb/c (bottom) mice were treated with 4 courses of the standard dose of αCTLA-4 or the matched isotype IgG (100 μg) and $4PD1^{hi}$ were monitored in tumor and spleen after the 2^{nd} (C2) and the 4^{th} (C4) administration (TUBO-bearing mice; mean ± SEM; n=5; unpaired t test) or at the end of treatment (naive mice; mean ± SEM; n=4-5; unpaired t test). (E) Changes in circulating $4PD1^{hi}$ in an independent cohort of melanoma patients treated with pembrolizumab (pembro). Circulating $4PD1^{hi}$ and Treg frequencies among $CD4^+$ T cells and modulation relative to baseline (Post/Pre-Tx) in advanced melanoma patients during pembrolizumab treatment (2mg/kg, q3wks; mean ± SEM; n=18; paired t test) (Huang et al., 2017). (F) Analysis of cross-reactivity between therapeutic and detection anti-mouse PD-1 Abs. PD-1 expression in mouse spleen-derived $CD4^+$ T cells pre-incubated with or without the therapeutic anti-mouse PD-1 Ab used in this study (RMP1-14), as revealed by FACS with the APC-conjugated anti-PD-1 Ab RMP1-30 (left) or with the rabbit anti-PD-1 polyclonal Ab (poAb), used in immunofluorescent stainings (IF), followed by a proper FITC-labeled secondary Ab (right). * = $p<0.05$, ** = $p<0.01$, *** = $p<0.001$.

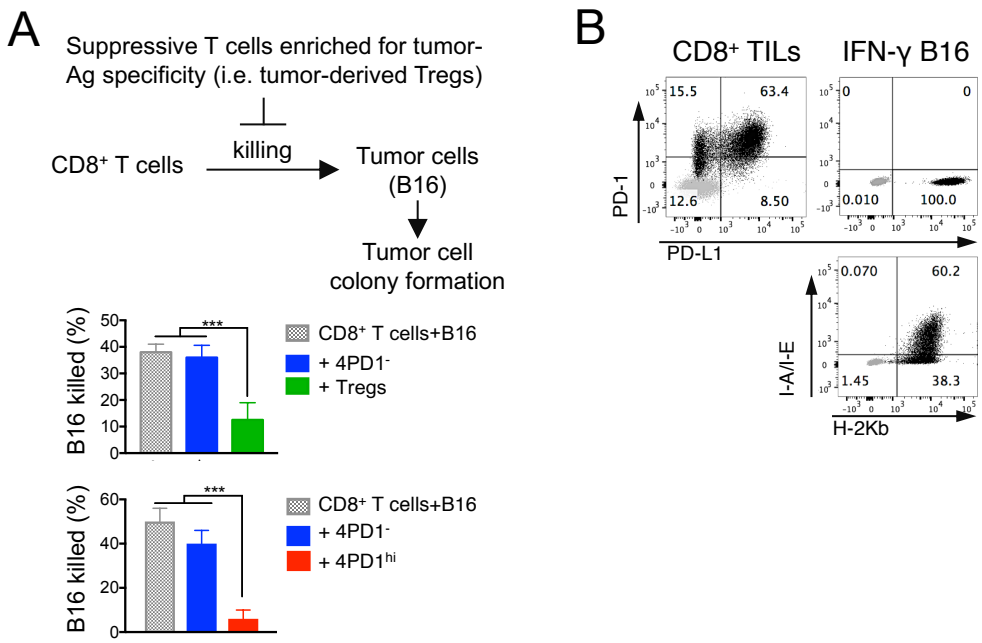

Figure S5. Related to Figure 5. Effects of Tregs and 4PD1^{hi} in 3D killing assay. (A) Inhibition of CD8$^+$ T-cell-mediated tumor killing by suppressive T cells in a 3D killing assay. In this assay, tumor-antigen specific CD8$^+$ T cells are co-cultured with tumor cells and suppressive T cells enriched for tumor-antigen specificity (i.e. tumor-derived Tregs) for 48 hr in order to evaluate the inhibition of CD8$^+$ T-cell-mediated tumor killing. Bar graphs show percent killed B16 cells in co-cultures with tumor-specific CD8$^+$ T cells (tumor-antigen specific, top; CD8 TILs, bottom) and tumor-derived Tregs (top) or 4PD1^{hi} (bottom) in comparison with 4PD1$^-$ (mean ± SD; top, n=3 with CD8$^+$ T cells alone and 4PD1$^-$, n=6 with Tregs; bottom, n=3 with 4PD1^{hi}, n=4 with CD8$^+$ T cells alone, n=5 with 4PD1$^-$; unpaired t test: *** = $p<0.001$). (B) B16 cells employed in 3D killing assays were pre-treated with IFN-γ to up-regulate MHC-I (H-2Kb) and MHC-II (I-A/I-E) and be recognized by both CD8$^+$ and CD4$^+$ T cells in culture. Representative FACS plots of the indicated markers in CD8$^+$ TILs and IFN-γ-pre-treated B16 (IFN-γ_B16) used in 3D killing assays. Ag, antigen.

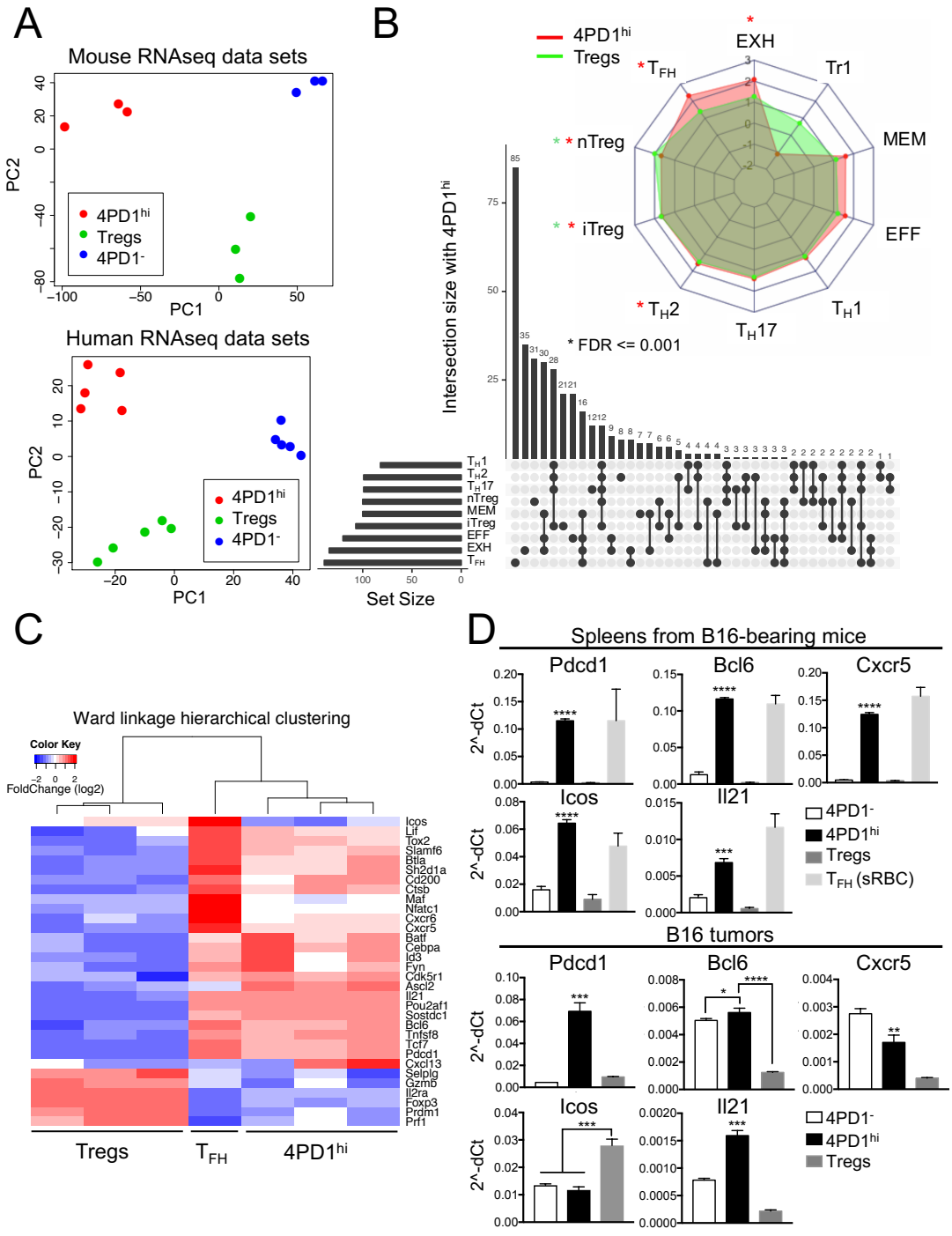
A
Mouse RNAseq data sets
PC2
PC1
4PD1hi
Tregs
4PD1-
Human RNAseq data sets
B
4PD1hi
Tregs
EXH
Tr1
MEM
EFF
TH1
TH17
TH2
TFH
nTreg
iTreg
* FDR <= 0.001
Intersection size with 4PD1hi
Set Size
C
Ward linkage hierarchical clustering
Color Key
FoldChange (log2)
Tregs
TFH
4PD1hi
D
Spleens from B16-bearing mice
Pdcd1
Bcl6
Cxcr5
Icos
Il21
2^-dCt
4PD1-
4PD1hi
Tregs
TFH (sRBC)
B16 tumors

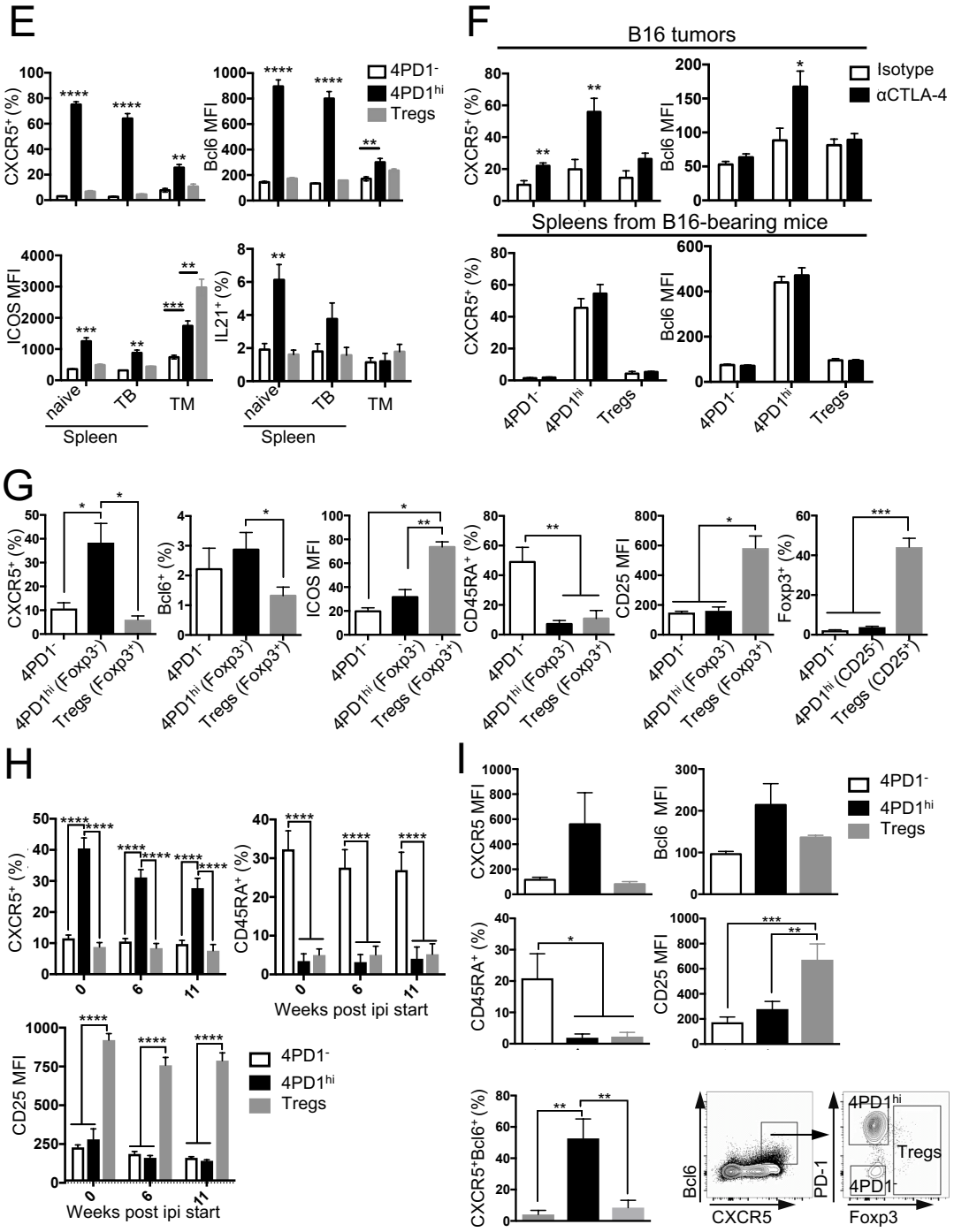
E
F
B16 tumors
Spleens from B16-bearing mice
4PD1-
4PD1hi
Tregs
Isotype
αCTLA-4
CXCR5+ (%)
Bcl6 MFI
ICOS MFI
IL21+ (%)
naive
TB
TM
Spleen
G
Bcl6+ (%)
CD45RA+ (%)
CD25 MFI
Foxp3+ (%)
4PD1- (Foxp3-)
4PD1hi (Foxp3-)
Tregs (Foxp3+)
4PD1hi (CD25+)
Tregs (CD25+)
H
Weeks post ipi start
I
CXCR5 MFI
CXCR5+Bcl6+ (%)
Bcl6
PD-1
CXCR5
Foxp3

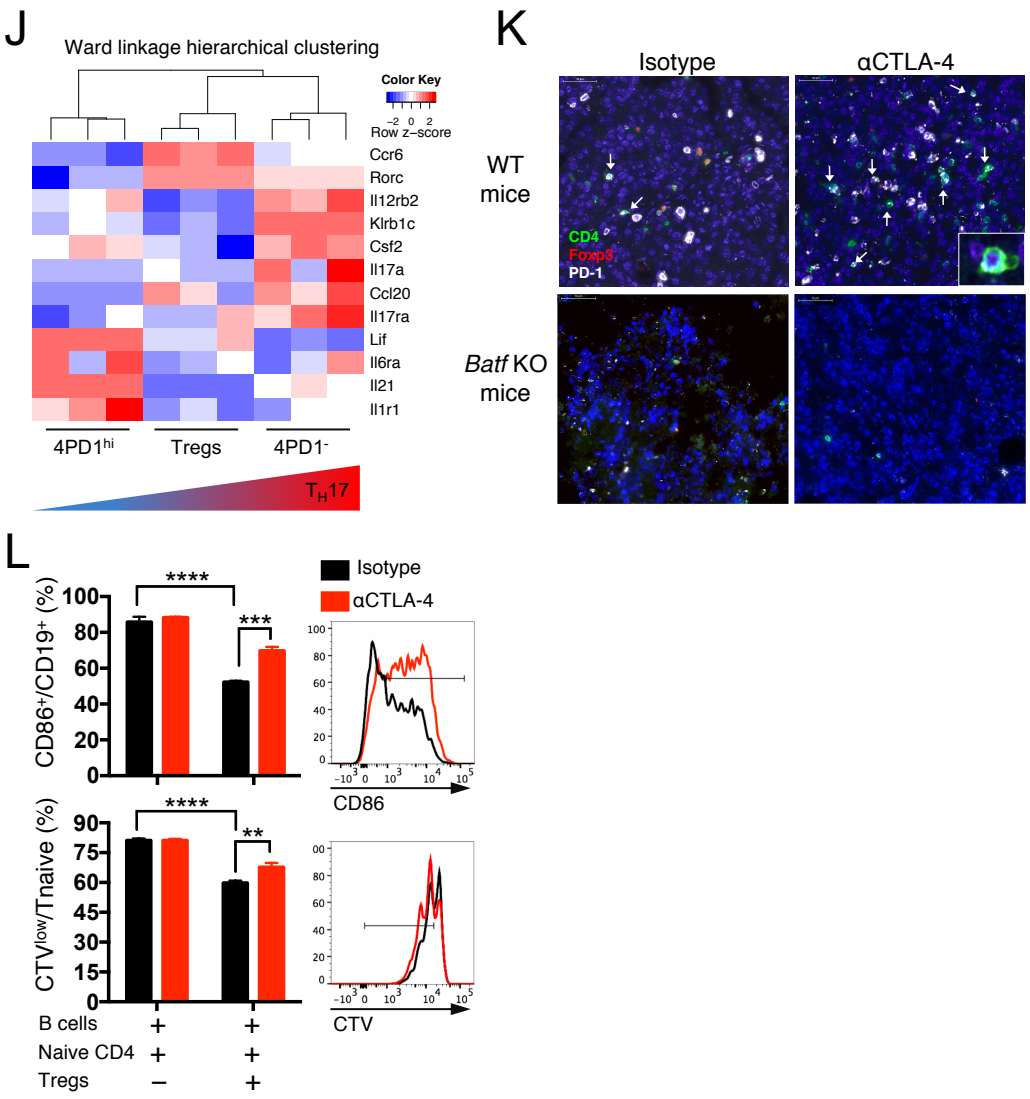

Figure S6. Related to Figure 6. T_{FH}-like phenotype in mouse and human 4PD1^{hi}. (A) Principal component analysis of variably expressed genes (sds>0.04, n=12,083, top) and differentially expressed genes (adjusted p value<0.05, n=2,059, bottom) in mouse splenic (top) and donor-derived (bottom) 4PD1^{hi}, 4PD1^{-} and Tregs. (B-F) T_{FH}-like phenotype expression by 4PD1^{hi} from naive and tumor-bearing mice. (B) Gene Set Enrichment Analysis (GSEA) of gene signatures from various CD4^{+} T-cell subsets in 4PD1^{hi} and Treg gene expression data sets generated in our study. Gene sets for T_H1, T_H2, T_H17, iTREG, and nTREG are from GSE14308, gene sets for EXH, MEM, EFF from GSE30431 and T_{FH} from GSE85316, and are all relative to naive T cells. Tr1 gene set is from GSE92940 and relative to Th0 cells. GSEA v2.2.4 was run with the following parameters: 1000 permutations gene set permutation type, using "weighted" enrichment statistic, and Signal2Noise as a metric for ranking genes. The leading-edge genes in each CD4^{+} T-cell gene set were compared to identify overlapping and unique genes. A spider plot depicting normalized enrichment scores from the GSEA and a bar plot depicting the overlaps of the various gene sets with 4PD1^{hi} data set are shown (B). EXH, exhausted CD4^{+} T cells; T_{FH}, follicular helper T cells; nTREG, natural regulatory T cells (Tregs); iTREG, inducible Tregs; T_H1, T helper 1; T_H2, T helper 2; T_H17, T helper 17; EFF, effector CD4^{+} T cells; MEM, memory CD4^{+} T cells; Tr1, type 1 Tregs. (C) Analysis of known T_{FH} differentially expressed genes (Choi et al., 2015; Kenefeck et al., 2015; Liu et al., 2012; Miyauchi et al., 2016; Table S2) in mouse 4PD1^{hi} and Treg data sets (A) in comparison with publicly available “bona fide” mouse T_{FH} gene expression

data(Miyauchi et al., 2016). Transcriptomes were normalized relative to the naive T-cell data set in each study to allow for a direct comparison. (D) mRNA expression of the indicated T_{FH}-associated genes by qPCR in splenic (top) and tumor-derived (bottom) 4PD1^{hi}, 4PD1^{-} and Tregs isolated from B16-bearing Foxp3-GFP transgenic mice (mean ± SD; n=3; unpaired t test, 4PD1^{hi} vs Tregs and 4PD1^{-} unless otherwise specified). Splenic T-cell subsets are compared with CXCR5^{+}PD-1^{hi}Foxp3^{-}CD4^{+} T_{FH} FACS-sorted from the spleen of Foxp3-GFP transgenic mice immunized with sRBC (mean ± SD, n=3). (E) Expression analyses by FACS of the indicated T_{FH}-associated markers in 4PD1^{hi}, 4PD1^{-} and Tregs from tumors (TM) and spleens of naive or B16 tumor-bearing (TB) mice (mean ± SEM; n=5; unpaired t test, 4PD1^{hi} vs Tregs and 4PD1^{-}). (F) CXCR5 and Bcl6 expression by FACS in tumor-derived (top) and splenic (bottom) 4PD1^{hi}, 4PD1^{-} and Tregs from B16-bearing mice treated with αCTLA-4 or control isotype IgG (100 µg) (mean ± SEM; n=5; unpaired t test, IgG vs αCTLA-4). (G-I) T_{FH}-like phenotype expression by donor- and patient-derived 4PD1^{hi}. (G) Expression analyses by FACS of the indicated T_{FH}, memory and Treg markers in donor-derived circulating 4PD1^{hi}, 4PD1^{-} and Tregs (mean ± SEM; n=3-6 depending on the marker; paired t test). Tregs and 4PD1^{hi} were gated as live single CD45^{+}CD4^{+}Foxp3^{+} (Tregs) and CD45^{+}CD4^{+}Foxp3^{-}PD-1^{hi} (4PD1^{hi}), or live single CD45^{+}CD4^{+}CD25^{+} (Tregs) and CD45^{+}CD4^{+}CD25^{-}PD-1^{hi} (4PD1^{hi}) to measure CD25 and Foxp3 expression respectively. (H) Frequency of CXCR5^{+} and CD45RA^{+} cells, and CD25 MFI in circulating 4PD1^{hi}, 4PD1^{-} and Tregs from advanced melanoma patients before and during ipilimumab treatment (3mg/kg, q3wks; mean ± SEM; n=15-20 depending on the time point; paired t test). (I) CXCR5, Bcl6 and CD25 MFI and CD45RA^{+} % in the indicated subsets gated on live single CD4^{+}CD45^{+} cells from immunotherapy-naive human melanoma lesions (top). Frequency of 4PD1^{hi}, 4PD1^{-} and Tregs within the CD4^{+}CXCR5^{+}Bcl6^{+} T_{FH} gate in the same samples and FACS plots depicting the gating strategy for this analysis (bottom) (mean ± SEM; n=10; paired t test). (J-L) αCTLA-4 increases T_{FH}-like 4PD1^{hi} and B-cell dependent T-cell priming. (J) Unsupervised hierarchical clustering with the related heatmap of $T_{H}17$-associated genes(Kenefeck et al., 2015) in gene expression data sets from functionally validated mouse splenic 4PD1^{hi}, 4PD1^{-} and Tregs (A, top). (K) Representative immunofluorescent stainings of CD4 (AlexaFluor488, green), Foxp3 (AlexaFluor568, red) and PD-1 (AlexaFluor647, white) in tumor tissue sections from B16-bearing WT and *Batf* knockout (KO) mice treated with αCTLA-4 (100 µg) or control isotype IgG (scale bar, 50µm; 40x original magnification; inset, 60x original magnification) as quantified in Figure 6C. Arrows indicate 4PD1^{hi} in tumors from WT mice. (L) CD86 expression in CD45.1^{+}CD19^{+} B cells (top) and proliferation (CTV^{low}) of target naive CD4^{+} T cells (bottom) co-cultured with or without Tregs in the presence of αCTLA-4 or control isotype IgG for 48 hr (mean ± SD; n=3; unpaired t test). Representative plots from B cells+Tregs+CD4 co-cultures treated with αCTLA-4 or control isotype IgG are shown. * = $p<0.05$, ** = $p<0.01$, *** = $p<0.001$, **** = $p<0.0001$.

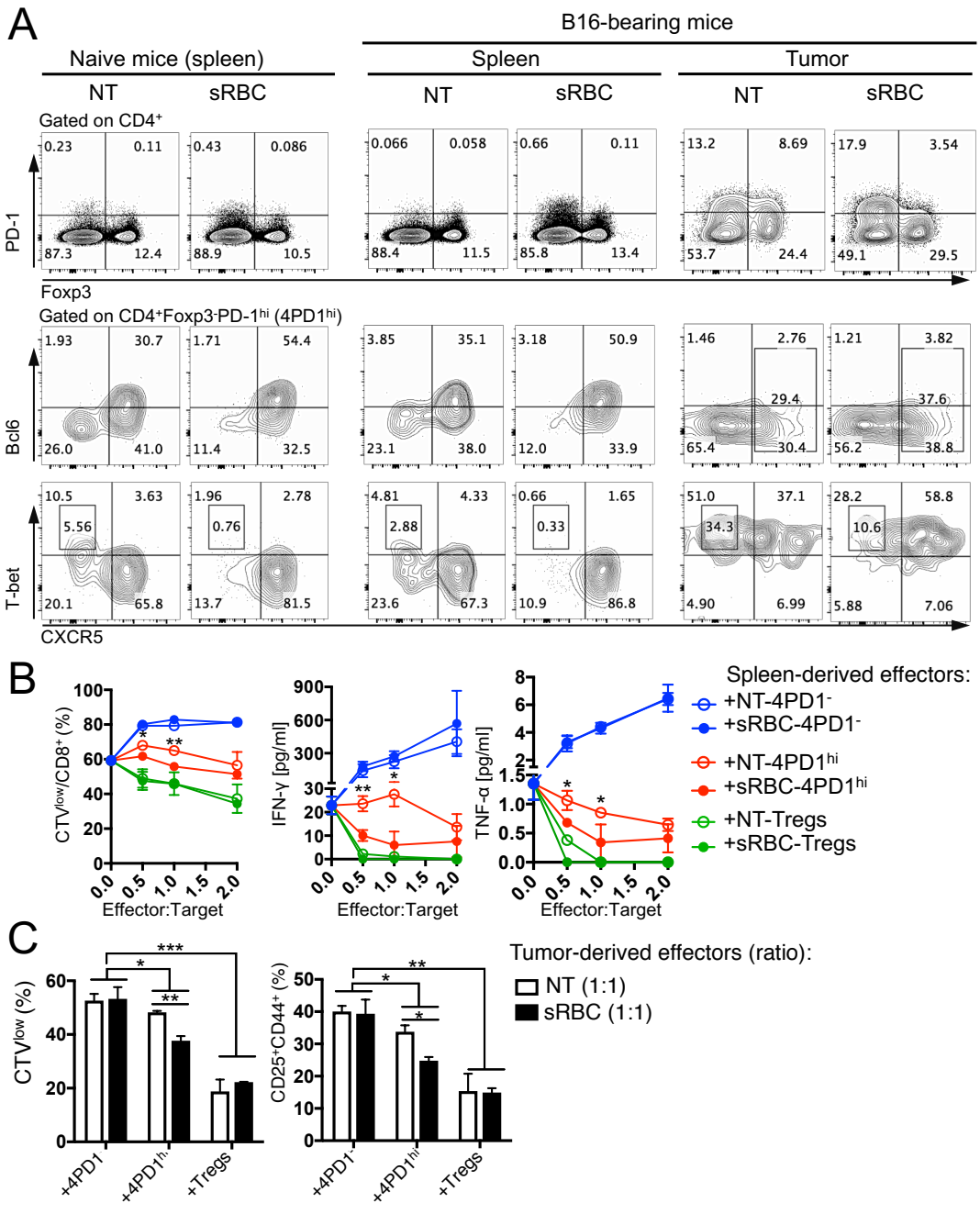
A
B16-bearing mice
Naive mice (spleen)
Spleen
Tumor
NT
sRBC
NT
sRBC
NT
sRBC
Gated on CD4+
PD-1
Foxp3
Gated on CD4+Foxp3-PD-1hi (4PD1hi)
Bcl6
T-bet
CXCR5
B
CTVlow/CD8+ (%)
IFN-γ [pg/ml]
TNF-α [pg/ml]
Effector:Target
Spleen-derived effectors:
+NT-4PD1-
+sRBC-4PD1-
+NT-4PD1hi
+sRBC-4PD1hi
+NT-Tregs
+sRBC-Tregs
C
CTVlow (%)
CD25+CD44+ (%)
+4PD1-
+4PD1hi
+Tregs
Tumor-derived effectors (ratio):
NT (1:1)
sRBC (1:1)

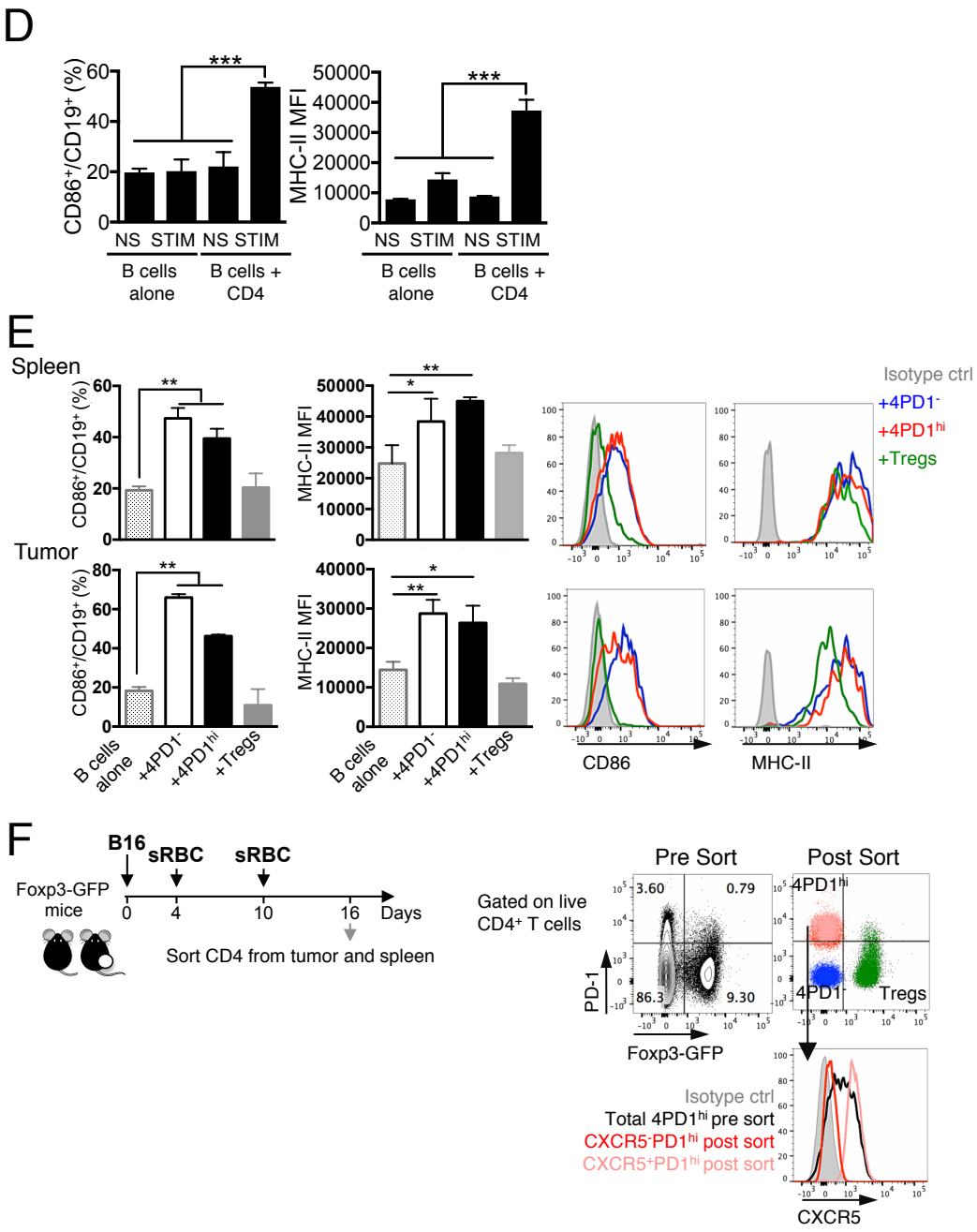
D
CD86+/CD19+ (%)
MHC-II MFI
***
NS STIM NS STIM
B cells alone
B cells + CD4
E
Spleen
Tumor
Isotype ctrl
+4PD1-
+4PD1hi
+Tregs
B cells alone
CD86
MHC-II
F
B16
sRBC
sRBC
Foxp3-GFP mice
0 4 10 16 Days
Sort CD4 from tumor and spleen
Gated on live CD4+ T cells
Pre Sort
Post Sort
3.60
0.79
86.3
9.30
4PD1hi
4PD1-
Tregs
PD-1
Foxp3-GFP
Isotype ctrl
Total 4PD1hi pre sort
CXCR5-PD1hi post sort
CXCR5+PD1hi post sort
CXCR5

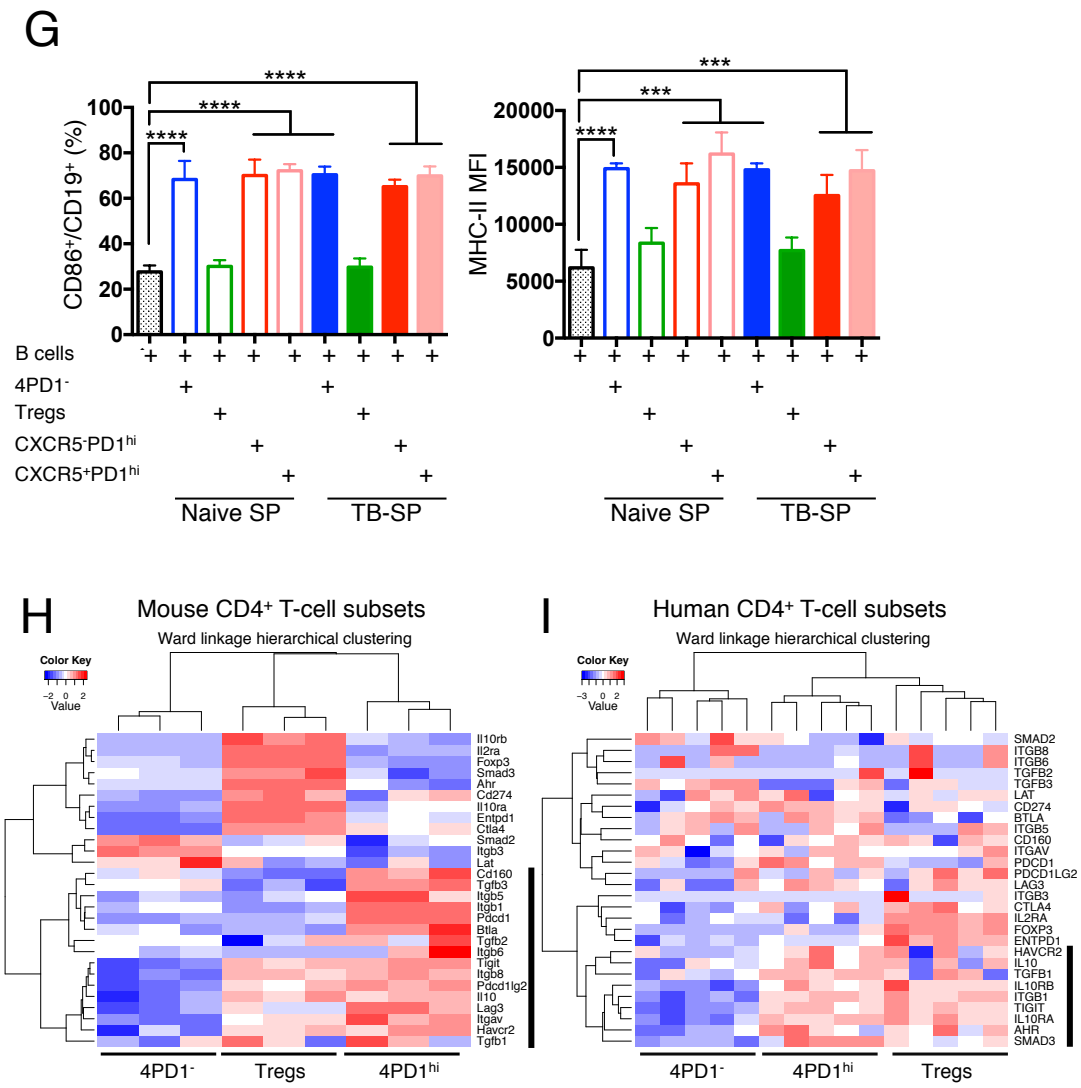

Figure S7. Related to Figure 7. Functional activity of T_{FH}-like 4PD1^{hi}. (A-C) 4PD1^{hi} phenotypic and functional modulation by sRBC immunization. (A) Representative FACS plots showing modulation of 4PD1^{hi} % and CXCR5, Bcl6, and T-bet expression in 4PD1^{hi} from naive and B16-bearing mice one week after immunization with sRBC in comparison with untreated mice (NT). Increased Bcl6 and/or CXCR5 expression and reduced Bcl6^{-}CXCR5^{-} and Tbet^{+}CXCR5^{-} cell proportion within 4PD1^{hi} from both spleens and tumors in naive and B16-bearing mice immunized with sRBC indicate T_{FH} differentiation. (B,C) 4PD1^{hi}, 4PD1^{-} and Tregs were FACS-sorted from spleens (B) or tumors (C) of non-treated (NT) or sRBC-immunized B16-bearing Foxp3-GFP transgenic mice as shown in Figure 7A and tested in suppression assays at the indicated effector:target ratios. Proliferation of CD45.1^{+}CD8^{+} target T cells (CTV^{low}) cultured with the indicated spleen-derived CD4^{+} T-cell subsets and quantification by Luminex-based bead immunoassay of IFN-γ and TNF-α in culture supernatants after 48-hr incubation (mean ± SD; n=3; unpaired t test, NT-4PD1^{hi} vs sRBC-4PD1^{hi}) (B). (C) Proliferation (CTV^{low}) and activation (CD25^{+}CD44^{+}) of CD45.1^{+}CD4^{+} target T cells co-cultured at 1:1 ratio with the indicated tumor-derived CD4^{+} T-cell subsets for 48 hr (mean ± SD; n=2-3; unpaired t test). (D-G) Effects of 4PD1^{hi} in T-cell dependent B-cell activation assay. (D) Culture stimulation conditions used in B-cell activation assays for the detection of T-cell-mediated effects on B cell activation. CD19^{+}CD4^{-}CD45.1^{+} B cells were cultured alone (B cells alone) or with CD45.1^{-}CD4^{+} T cells (B cells + CD4) at 2:1 ratio and stimulated (STIM) or not (NS) with PHA+IL-

2. After 48-hr incubation, percent of $CD86^+$ and MHC-II MFI in total B cells were quantified by FACS (mean ± SD; n=3; unpaired t test). In these conditions, activation of B cells is observed only when they are stimulated in the presence of T cells (T-cell dependent B-cell activation). (E) B-cell activation assays with $4PD1^{hi}$, $4PD1^-$ and total Tregs FACS-sorted from spleens (top) or tumors (bottom) of untreated B16-bearing Foxp3-GFP mice. Representative FACS plots and quantification of percent $CD86^+$ (average ± SEM; n=2 independent experiments with tumor-derived T cells, n=3 independent experiments with spleen-derived T cells; unpaired t test) and MHC-II MFI (average ± SD; n=3-5 replicates from one representative experiment; unpaired t test) within $CD19^+CD4^-CD45.1^+$ target B cells stimulated alone or with the indicated $CD4^+$ T-cell subsets for 48 hr. (F,G) Naive and B16-bearing mice were immunized with sRBC and $CXCR5^+$ and $CXCR5^-$ $4PD1^{hi}$ were sorted from spleens and tumors along with $4PD1^-$ and total Tregs (F) and tested in B-cell activation assays (G). (G) $CD86^+$ cell % and MHC-II MFI in target $CD45.1^+CD4^-CD19^+$ B cells stimulated in culture with the indicated $CD4^+$ T-cell subsets for 48 hr (mean ± SD; n=4-6; unpaired t test). (H,I) Unsupervised hierarchical clustering with the related heatmaps of immune inhibitory genes (Table S2) in RNAseq data sets from mouse splenic (H) and donor-derived (I) $4PD1^{hi}$, $4PD1^-$ and Tregs (Figure S6A). Genes overexpressed in $4PD1^{hi}$ are highlighted with a black line. * = $p<0.05$, ** = $p<0.01$, *** = $p<0.001$, **** = $p<0.0001$.

Supplemental Tables

Table S1

Family	Sequence 5'–3'		Estimated Product Size
MuBV1	CTGAATGCCCAGACAGCTCCAAGC	1	170
MuBV2	TCACTGATACGGAGCTGAGGC	2	161
MuBV3.1	CCTTGCAGCCTAGAAATTCAGT	3	150
MuBV4	GCCTCAAGTCGCTTCCAACCTC	4	189
MuBV5.1	CATTATGATAAAATGGAGAGAGAT	5	222
MuBV5.2	AAGGTGGAGAGAGACAAAGGATTC	6	213
MuBV5.3	AGAAAGGAAACCTGCCTGGTT	7	200
MuBV6	CTCTCACTGTGACATCTGCCC	8	143
MuBV7	TACAGGGTCTCACGGAAGAAGC	9	177
MuBV8.1	CATTACTCATATGTCGCTGAC	10	228
MuBV8.2	CATTATTCATATGGTGCTGGC	11	228
MuBV8.3	TGCTGGCAACCTTCGAATAGGA	12	214
MuBV9	TCTCTCTACATTGGCTCTGCAGGC	13	144
MuBV10	ATCAAGTCTGTAGAGCCGGAGGA	14	135
MuBV11	GCACTCAACTCTGAAGATCCAGAGC	15	151
MuBV12	GATGGTGGGGCTTTCAAGGATC	16	204
MuBV13	AGGCCTAAAGGAACTAACTCCCAC	17	165
MuBV14	ACGACCAATTCATCCTAAGCAC	18	155
MuBV15	CCCATCAGTCATCCCAACTTATCC	19	174
MuBV16	CACTCTGAAAATCCAACCCAC	20	145
MuBV17	AGTGTTCCTCGAACTCACAG	21	167
MuBV18	CAGCCGGCCAAACCTAACATTCTC	22	169
MuBV19	CTGCTAAGAAACCATGTACCA	23	161
MuBV20	TCTGCAGCCTGGGAATCAGAA	24	149
Constant Primers			
MuTCB3C	GCCAGAAGGTAGCAGAGACCC		
MuTCB1up	GAGAAATGTGACTCCACCCAA		
MuTCB1-FAM	FAM-(C)TTGGGTGGAGTCACATTTCTC		
MuTCB1-HEX	HEX-(C)TTGGGTGGAGTCACATTTCTC		

Table S1. Related to Figure S1E and the STAR Methods section. Primers used for spectratyping analyses.

Table S2

T_{FH} differentially expressed gene names	Immunosuppressive gene names
Ascl2	BTLA
Batf	CD160
Bcl6	CTLA4
Btla	FOXP3
Cd200	HAVCR2
Cdk5r1	AHR
Cebpa	IL10
Ctsb	IL10RA
Cxcl13	IL10RB
Cxcr5	LAG3
Cxcr6	PDCD1
Foxp3	PDCD1LG2
Fyn	CD274
Gzmb	TGFB1
Icos	TGFB2
Id3	TGFB3
Il21	SMAD2
Il2ra	SMAD3
Lif	LAT
Maf	ITGAV
Nfatc1	ITGB1
Pdcd1	ITGB3
Pou2af1	ITGB5
Prdm1	ITGB6
Prf1	ITGB8
Selplg	ENTPD1
Sh2d1a	TIGIT
Slamf6	IL2RA
Sostdc1	
Tcf7	
Tnfsf8	
Tox2	

Table S2. Related to Figure S6C and S7H,I and the STAR Methods section. T_{FH} differentially expressed genes tested in mouse $4PD1^{hi}$, Tregs and conventional T_{FH} RNAseq data sets and immunosuppressive genes analyzed in RNAseq data sets from mouse and human $CD4^{+}$ T-cell subsets.